Proteinase-Activated Receptor 4 (PAR4) Activation Triggers Cell Membrane Blebbing through RhoA and β-arrestin.

Christina MG Vanderboor, Pierre E Thibeault, Kevin CJ Nixon, Robert Gros, Jamie Kramer and Rithwik Ramachandran.
Department of Physiology and Pharmacology, Schulich School of Medicine and Dentistry, University of Western Ontario, London, Ontario, Canada.

Correspondence and request for materials should be directed to:

Rithwik Ramachandran,
Department of Physiology and Pharmacology,
Schulich School of Medicine and Dentistry,
University of Western Ontario, London,
Ontario, Canada.
519-661-2142
rramach@uwo.ca

Abstract

Proteinase-Activated Receptors (PARs) are a four-member family of G-protein coupled receptors that are activated via proteolysis. PAR4 is a member of this family that is cleaved and activated by the serine proteinases such as thrombin, trypsin and cathepsin-G. PAR4 is expressed in a variety of tissues and cell types including the platelets, vascular smooth muscle cells and neuronal cells. In studying PAR4 signaling and trafficking, we observed dynamic changes in the cell membrane with spherical membrane protrusions that resemble plasma membrane blebbing. Since non-apoptotic membrane blebbing is now recognized as an important regulator of cell migration, cancer cell invasion, and vesicular content release we sought to elucidate the signaling pathway downstream of PAR4 activation that leads to such events. Using a combination of pharmacological inhibition and CRISPR/Cas9 mediated gene editing approaches we establish that PAR4-dependent membrane blebbing occurs independently of the $G\alpha_{q/11}$ and $G\alpha_i$ signaling pathways and is dependent on signaling via the β-arrestin-1/-2 pathway and RhoA signaling. In order to gain a more comprehensive understanding of β-arrestin mediated signaling downstream of PAR4 and to guide future studies, we undertook RNAseq analysis of PAR4 activated genes in control cells and in cells lacking β-arrestin-1/-2. A list of differentially expressed genes was generated followed by Gene Ontology (GO) and enrichment analysis revealing PAR4 regulation of genes involved in processes including blood coagulation and circulation, cell-cell adhesion, sensory perception and neuron-neuron synaptic transmission, terms that relates back to known function of PAR4 and that are consistent with our finding of membrane blebbing triggered by PAR4 activation. Together these studies provide further mechanistic insight into PAR4 regulation of cellular function.

Introduction

Proteinase activated receptors (PARs) are a four-member family of G-protein coupled receptors (GPCRs). PARs are unique among GPCRs, in being activated via proteolytic unmasking of a receptor activating 'tethered ligand', that interacts intramolecularly with the orthosteric ligand binding pocket to trigger signaling (Ramachandran *et al.*, 2012) . PAR4, the most recently identified member of this family (Xu *et al.*, 1998), is expressed in a variety of tissues and cell types including the platelets, vascular smooth muscle cells, neuronal cells, and some cancer cells.

Much work has been done to develop PAR1- and PAR4-targeted compounds as anti-platelet agents. Both PAR1 and PAR4 are expressed in human platelets and both of these receptors are activated by the coagulation cascade enzyme thrombin. Importantly though, PAR1 and PAR4 appear to serve different roles in the platelet activation process (Kahn *et al.*, 1999), with PAR1 the high affinity thrombin receptor playing an initiating role and the lower affinity thrombin receptor PAR4 serving to consolidate and propagate the clot (Kahn *et al.*, 1999). The PAR1 antagonist voropaxar (zontivity), while highly effective in reducing cardiovascular complications, exhibited significant side effects with an elevated risk for bleeding including in the brain (Morrow *et al.*, 2012), further spurring recent efforts to target PAR4. Recent work with small molecule PAR4 antagonists has supported the idea that PAR4 antagonists are effective in reducing platelet rich thrombus formation in human platelets *ex-vivo* (Wilson *et al.*, 2017) and in rodent and non-human primate models *in-vivo* (Wong *et al.*, 2017). In non-human primate models, PAR4 blockade was associated with low bleeding liability and had a markedly wider therapeutic window compared to the commonly used antiplatelet agent clopidogrel (Wong *et al.*, 2017).

In keeping with emerging literature for other GPCRs, we now know that activated PAR4 can directly couple to multiple G-protein signaling pathways including $G\alpha_{q/11}$ and the $G\alpha_{12/13}$ pathway (Woulfe, 2005; Kim *et al.*, 2006) but is thought not to engage $G\alpha_i$ dependent signaling pathways (Kim *et al.*, 2006). PAR4 can also recruit and signal through β-arrestins (Li *et al.*, 2011; Ramachandran *et al.*, 2017). In recent work, we identified a C-terminal motif in PAR4 that was critical for PAR4 signaling through the $G\alpha_{q/11}$ calcium signalling pathway and for recruiting β-arrestin-1/-2 (Ramachandran *et al.*, 2017). The mutant receptor with an 8-amino acid C-terminal deletion (dRS-PAR4) failed to internalize following activation with the PAR4 agonists thrombin or AYPGKF-NH_2 suggesting a role for β-arrestins in PAR4 trafficking. A pepducin targeting this C-terminal motif was also effective in attenuating PAR4 dependent platelet aggregation and thrombosis *in-vivo* (Ramachandran *et al.*, 2017). These recent findings point to the exciting possibility that it might be possible to therapeutically target PAR4 signaling in a pathway specific manner. The present study was spurred by our observations that PAR4 activation rapidly triggered the formation of dynamic membrane blebs, which were absent in dRS-PAR4 expressing cells.

Non-apoptotic plasma membrane blebbing is now recognized as a feature of various cellular processes including directional cellular migration during development, cancer cell migration and invasion, neuronal cell remodeling, and vesicular content release (Charras, 2008; Charras and Paluch, 2008; Charras *et al.*, 2008). Blebs are formed when the plasma membrane transiently detaches from the underlying actin filaments resulting in intracellular pressure-mediated spherical membrane protrusions (Charras *et al.*, 2008; Tinevez *et al.*, 2009). The reassembly of actin filaments limits the expansion of blebs and actin

polymerization while actomyosin contraction drives the retraction of the blebs (Charras *et al.*, 2008). The molecular signals that trigger the formation of membrane blebs are begining to be understood and include signalling from cell surface receptor such as GPCRs and receptor tyrosine kinases (Hagmann *et al.*, 1999; Lawrenson *et al.*, 2002; Godin and Ferguson, 2010; Chen *et al.*, 2012; Laser-Azogui *et al.*, 2014). A role for multiple Rho isoforms has also been described in regulating various aspects of bleb formation and retraction (Pinner and Sahai, 2008; Aoki *et al.*, 2016; Gong *et al.*, 2018). Previous work has described regulation of Rho signaling by GPCRs in both a G-protein- and β-arrestin-dependent manner (Sah *et al.*, 2000; Barnes *et al.*, 2005; Anthony *et al.*, 2011).

Here we examine in detail the pathways leading from PAR4 to the formation of membrane blebs. We find that inhibition of $G\alpha_{q/11}$ signaling had no effect on the formation of PAR4 triggered membrane blebs, while blockade of β-arrestin-1/-2 or Rho-dependent signaling significantly reduced blebbing.

Materials and Methods

Materials

DMEM, trypsin-EDTA, PBS, Penicillin-Streptomycin and sodium pyruvate were purchased from Thermo Fisher (Waltham, MA). Peptide ligands were custom synthesized by Genscript (Piscataway, NJ) at greater than 95% purity. Thrombin was purchased from Calbiochem (Oakville, ON), coelanterazine-h was from Nanolight Technology (Pinetop, AZ). All antibodies (anti-β-arrestin-1/-2, anti-RhoA, anti-actin, anti-rabbit-HRP) used in this study were purchased from Cell Signaling Technologies. YM254890 was from Wako chemicals (Richmond, VA), GSK269962 was from Tocris (Oakville, ON) and all other chemicals were from Sigma-Aldrich (Oakville, ON).

Cell Culture and transfections

HEK-293 (ATTC) cells were maintained in DMEM (Gibco) with 10% fetal bovine serum (Gibco), 1% penicillin-streptomycin (Gibco) and 1% sodium pyruvate (Gibco). Cells stably expressing PAR4-YFP or PAR4-dRS-YFP were maintained in the above media supplemented with 600 μg/mL of geneticin (Gibco). Cells were transiently transfected using a modified calcium phosphate method (Ferguson and Caron, 2004). Experiments were performed 48 hours post transfection. Primary rat smooth muscle cells were isolated and cultured as previously described (Gros Robert *et al.*, 2006).

Creation of β-arrestin-1/-2 and RhoA knockout cells.

RhoA and Arrestin-1/-2 knock out HEK-293 cells (RhoA-KO HEK and β-arrestin-1/-2-KO HEK respectively) were generated using CRISPR/Cas9 mediated gene targeting. Guides targeting the β-arrestins or RhoA were designed using the design tool at http://crispr.mit.edu. Gene specific guides (β-arrestin 1; TGTGGACCACATCGACCTCG, β-arrestin 2; GCGGGACTTCGTAGATCACC and RhoA; CGAGTTTGCGACTCGCGGAC, CGGTCCGCGAGTCGCAAACT, GAGTCCAGCCTCTTCGCGCC, GACTCGCGGACCGGCGTCCC) were ligated into the PX458 vector (a kind gift from Dr. Feng Zhang, MIT, Addgene plasmid # 48138), verified by direct sequencing and transfected in HEK cells via the calcium phosphate method. 48 hours post transfection, GFP expressing single cells were flow sorted into individual wells

140 of a 96 well (Becton Dickinson FACSAria III). Clonal cells from individual wells were
141 screened by western blotting to identify cell lines which were deficient in β-arrestin 1/2 or
142 RhoA (Supplementary Figure 1).
143
144 **Confocal microscopy**
145 Cells were plated onto glass bottom 35 mm dishes (MatTek, Ashland, MA) and imaged
146 using Zeiss LSM 510 Meta NLO confocal microscope. Yellow fluorescent protein was
147 excited with 514 laser line and visualized with 535-560 filter set. mCherry fluorophore was
148 excited with 543 laser line and visualized with 560-590. Green fluorescent protein was
149 excited with 488 laser line and visualized with 530-560 filter set. Cell shape change
150 experiments were conducted as follows. Cells were treated with vehicle or inhibitor as
151 indicated in the figure legends and incubated at 37°C. Plates were then placed on a heated
152 stage on the microscope and PAR4 was activated with AYPGKF-NH_2 (30μM) or thrombin
153 (3U/ml). 6-12 images per dish were taken over 10 minutes. Images were analyzed by
154 manually counting cells displaying membrane protrusions or blebs versus cells that did not
155 display any membrane protrusions.
156
157 **Bioluminescent Resonance Energy Transfer (BRET) assay for β-arrestin-1/-2**
158 **recruitment.**
159 Bioluminescent resonance energy transfer was measured between c-terminally YFP tagged
160 PAR4 (Ramachandran *et al.*, 2017) and Renilla Luciferase (Rluc) tagged β-arrestin 1 or β-
161 arrestin 2 (a kind gift from Dr. Michel Bouvier, U de Montreal), following 20 minutes of
162 receptor activation as described in previous studies (Ramachandran *et al.*, 2009). Briefly,
163 PAR4-YFP (1 μg) and Rluc-β-arr1 and 2) (0.1μg) were transiently transfected in cells
164 plated in a six well plate for 24 hours. Cells were re-plated into white 96-well culture plates
165 and cultured for a further 24 hours. Interactions between PAR4 and β-arrestin-1/-2 were
166 detected by measuring the BRET ratio at timed intervals over 20 min following the addition
167 of 5 μM coelenterazine (Nanolight Technology, Pinetop, AZ) on a Mithras fluorescence
168 plate reader (Berthold) in luminescence mode using the appropriate filters.
169
170 **RNASeq PAR4 transcriptome analysis in control and β-arrestin 1/2 knockout HEK-**
171 **293 cells.**
172 HEK-293 cells or β-arrestin-1/-2-KO HEK cells stably expressing PAR4-YFP were treated
173 with 30μM AYPGKF-NH2 for 2 hours. RNA was extracted using an RNeasy mini kit
174 (Qiagen) and analyzed on a bioanalyzer (Agilent, Santa Clara, CA). Sequencing libraries
175 were generated using the ScriptSeq complete kit which incorporated the Ribo-Zero
176 ribosomal RNA (rRNA) removal technology. Sequencing was done on a NextSeq
177 (Illumina) at the London Regional Genomics Centre.
178
179 **Sequencing Analysis**
180 Raw sequencing reads were trimmed using Prinseq quality trimming (Schmieder and
181 Edwards, 2011) with a minimum base quality score of 30. Read quality was then assessed
182 using FastQC (http://www.bioinformatics.babraham.ac.uk/projects/fastqc). Trimmed reads
183 were then aligned to the *Homo sapiens* reference genome (CRCh release 38) using the
184 STAR RNA-Seq aligner (Dobin *et al.*, 2013). An average of 28,049,697 and 20,706,493
185 high quality uniquely aligned reads with a maximum of four mismatches were obtained

186 from HEK-293 cells and β-arr-1/-2-KO-HEK cells respectively. (Table 1 and Figure S2 and
187 S3). The number of reads per gene was quantified by inputting reads that uniquely aligned
188 to the reference genome with a maximum of four mismatches into HTSeq-count (Anders *et*
189 *al.*, 2015) with the - type flag indicating 'gene' (Table 1 and Figure S2 and S3). Genes
190 associated with rRNA and non-protein coding genes were removed from the analysis and
191 genes with no reads across all samples in the count tables were removed from analysis
192 leaving 18,615 genes for downstream analysis. Raw gene counts were normalized and
193 differential expression analysis between HEK-293 cells and β-arr-1/-2-KO-HEK cells with
194 and without the treatment of 30μM AYPGKF-NH_2 was performed using the R (R: A
195 language and environment for statistical computing. Vienna, Austria: R Foundation for
196 Statistical Computing; 2017) package DESEQ2 (Love *et al.*, 2014). Differentially
197 expressed genes were defined as genes with a fold-change >2 and a Benjamini-Hochberg
198 adjusted p-value <0.05. Overlap between datasets was determined and visualized as a Venn
199 diagram using BioVenn (Zhang *et al.*, 2009). Gene ontology (GO) enrichment analysis was
200 performed on upregulated and downregulated differentially expressed genes with the
201 Panther software (Mi *et al.*, 2017) on http://geneontology.org using the GO-SLIM function.
202
203 **Accession numbers**
204 The raw data for RNA-seq is available at the NCBI Gene Expression omnibus (GEO),
205 accession number GSE134713.
206
207 **Statistical Analysis.** Statistical analysis of data and curve fitting were done with Prism 7
208 software (GraphPad Software, San Diego, CA). Statistical significance was assessed using
209 the Student's t-test or Anova with Tukey's post-test.
210
211 **Results**
212 **Activation of PAR4 elicits cell shape changes that are dependent on a c-terminal eight-**
213 **amino acid sequence.**
214 Stimulation of plasma membrane localized PAR4-YFP in HEK-293 cells stably
215 expressing PAR4-YFP with the PAR4 specific peptide agonist AYPGKF-NH_2 resulted in
216 cell shape changes (Fig. 1A, B). PAR4 expressing cells treated with 30 μM AYPGKF-
217 NH_2, displayed protrusions forming at the plasma membrane, indicated by arrows (Fig.
218 1B). These structures resemble membrane blebs and began to form around 2 minutes post
219 agonist stimulation and lasted for up to 30 minutes in the presence of 30 μM AYPGKF-
220 NH_2. In order to further verify that the cytoskeletal changes were indeed membrane blebs,
221 we examined the effect of treating cells with Blebbistatin, a small molecule inhibitor of
222 myosin II ATPase (Cheung *et al.*, 2002; Straight *et al.*, 2003) which functions by locking
223 actin heads in a low actin affinity complex (Kovács *et al.*, 2004) and is reported to inhibit
224 non-apoptotic membrane blebbing. Incubation of cells with blebbistatin significantly
225 reduced the AYPGKF-NH_2 stimulated membrane bleb response in PAR4-YFP expressing
226 HEK-293 cells (15.37% +/- 4.14) (Fig. 1C-E) . In contrast, PAR4-YFP expressing cells
227 treated with DMSO vehicle control displayed membrane blebs with a mean of 82.25% +/-
228 8.25. In recent studies we described a mutant PAR4 receptor lacking eight amino acids
229 from the c-tail, dRS-PAR4-YFP (Ramachandran *et al.*, 2017). We observed that in contrast
230 to the wild type receptor, dRS-PAR4-YFP expressing cells display significantly less
231 blebbing in response to 30 μM AYPGKF-NH_2 treatment (Fig. 2A-C). 82.33% +/- 1.2 of

232 HEK-293 cells stably expressing wild type PAR4-YFP displayed membrane blebbing as
233 opposed to 8.2% +/- 2.35 dRS-PAR4-YFP expressing cells, indicating that PAR4 triggered
234 membrane blebbing required the activation of signaling pathways that are dependent on the
235 eight-amino acid sequence in the c-tail of PAR4. Previously, we established that dRS-
236 PAR4-YFP does not couple to $G\alpha_{q/11}$ and is unable to recruit β-arrestins in response to
237 thrombin or AYPGKF-NH_2 activation (Ramachandran *et al.*, 2017). Since this mutant
238 receptor is also unable to activate blebbing, we hypothesized that PAR4 cell shape changes
239 are $G\alpha_{q/11}$ and or β-arrestin dependent and examined the effect of blocking these pathways
240 on bleb formation.
241
242 **PAR4-mediated cell shape change is $G\alpha_{q/11}$ and $G\alpha_i$ independent**
243 In order to determine whether PAR4 triggered blebbing is $G\alpha_{q/11}$-dependent, we
244 treated cells with the potent and selective $G\alpha_{q/11}$ inhibitor YM-254890 (Taniguchi *et al.*,
245 2004). It is well established that GPCRs couple to $G\alpha_{q/11}$ to mobilize calcium and activate
246 protein kinase C (PKC) (Exton, 1996; Wettschureck and Offermanns, 2005). Activated
247 PKC translocation from the cytosol to the plasma membrane can be observed to monitor
248 this process (Dale *et al.*, 2001; Policha *et al.*, 2006). We employed this assay to visualize
249 the efficacy of YM-254890 in inhibiting $G\alpha_{q/11}$ signaling through PAR4. Cells were
250 transiently transfected with PAR4-mCherry and PKCβ1-GFP. PAR4 expression was
251 observed at the cell membrane and PKCβ1 expression was evident in the cytoplasm in
252 resting cells. Upon treatment with 30 μM AYPGKF-NH_2, PKCβ1-GFP translocated to the
253 membrane (Fig. 3A-C) and blebbing responses were seen as before. In cells treated with
254 100 nM YM-254890, PKCβ1-GFP failed to translocate to the membrane following
255 treatment with AYPGKF-NH_2. 100nM YM-254890 treated cells however maintained their
256 ability to bleb in response to AYPGKF-NH_2 (Fig. 3D-F). The role of $G\alpha_{q/11}$ in PAR4
257 mediated blebbing was further quantified in HEK-293 cells stably expressing PAR4-YFP
258 treated with either DMSO vehicle or YM-254890 prior to stimulation with 30 μM
259 AYPGKF-NH_2. Blebbing in vehicle treated cells was not significantly different from cells
260 treated with YM-254890, 81.0% +/- 4.5 and 77.0% +/- 2.5 respectively (Fig. 3G). This
261 data indicates that YM-254890 functionally blocks $G\alpha_{q/11}$ signaling as indicated by a lack
262 of PKCβ1 translocation but does not block cell shape changes mediate by PAR4 activation.
263 HEK-293 cells, transiently expressing PAR4-mCherry with PKCβ1-GFP, showed
264 that activation of PAR4-mCherry with AYPGKF-NH_2 causes a translocation of PKCβ1-
265 GFP from the cytosol to the plasma membrane (Fig. 4A, B). In contrast, HEK-293 cells
266 transiently expressing dRS-PAR4-mCherry with PKCβ1-GFP showed that activation of
267 dRS-PAR4-mCherry does not cause a redistribution of PKCβ1-GFP to the membrane (Fig.
268 4C, D). Although PKC activation is downstream of $G\alpha_{q/11}$, since dRS-PAR4 does not
269 activate PKC and does not elicit cell shape changes, we tested PKC for a potential role in
270 mediating PAR4 cell shape changes. HEK-293 cells stably expressing PAR4-YFP were
271 treated with the PKC inhibitor Gö6983 (Gschwendt *et al.*, 1996), prior to stimulation with
272 30 μM AYPGKF-NH_2 and visualization by confocal microscopy. There was no significant
273 difference in the number of DMSO vehicle treated cells displaying blebbing when
274 compared to cells treated with Gö6983 in response to AYPGKF-NH_2, 74.5% +/- 4.6 and
275 72.2% +/- 9.2 (Fig. 4G). This data then suggests that neither $G\alpha_{q/11}$ or PKC facilitate
276 PAR4 mediated cell shape changes.

277 After ruling out $G\alpha_{q/11}$ as a potential signaling partner for PAR4-mediated
278 membrane blebs, we tested $G\alpha_i$ recruitment as a potential regulator of these responses
279 through inhibition of $G\alpha_i$ signaling with pertussis toxin. HEK-293 cells stably expressing
280 PAR4-YFP were incubated with pertussis toxin (100 nM) for 18 hrs prior to stimulating the
281 cells with 30 μM AYPGKF-NH_2. We did not observe any reduction in the number of cells
282 that displayed blebbing when compared to cells incubated with vehicle control (saline),
283 76.3% +/- 4.7 and 78.0% +/- 3.4 respectively (Fig. 5A-C).
284
285 **PAR4-mediated cell shape change is RhoA and ROCK dependent.**
286 Since RhoA can be activated by a $G\alpha_{q/11}$ and β-arrestin-1 dependent mechanism
287 following activation of the angiotensin II type 1 receptor (Barnes *et al.*, 2005) and since
288 RhoA is also well-established as a regulator of actin cytoskeleton rearrangements (Barnes
289 *et al.*, 2005; Aoki *et al.*, 2016), we examined whether PAR4-mediated blebbing was RhoA
290 and ROCK dependent. Treatment of PAR4-YFP expressing HEK-293 cells with the ROCK
291 specific inhibitor GSK269962 (Stavenger *et al.*, 2007) significantly reduced the number of
292 blebbing cells. 72.53% +/- 6.24 of DMSO vehicle control treated cells displayed blebbing
293 while only 15.6% +/- 6.28 of cells treated with GSK269962 (100 nM) displayed bleb
294 formation in response to 30μM AYPGKF-NH_2 (Fig. 6A-C). To further confirm the role of
295 RhoA in PAR4-mediated changes in the plasma membrane, a RhoA knock out HEK-293
296 cell line (RhoA-KO-HEK-293) was created by use of CRISPR/Cas9 targeting. RhoA-KO-
297 HEK-293 cells and control HEK-293 cells were transiently transfected with PAR4-YFP,
298 stimulated with 30 μM AYPGKF-NH_2 and imaged by confocal microscopy (Fig. 6D-F).
299 75% +/- 7.8 of control HEK-293 cells expressing PAR4-YFP and treated with AYPGKF-
300 NH_2 displayed membrane blebbing while RhoA-KO-HEK-293 expressing PAR4-YFP
301 show significantly fewer cells with blebs in response to agonist (22.8% +/- 6.2) (Fig. 6F).
302 Taken together these data indicate that stimulation of PAR4-YFP elicits cell shape changes
303 that are blocked by blebbistatin and by the ROCK inhibitor GSK269962. Further, these
304 cell shape changes do not occur in cells that do not express RhoA protein, suggesting that
305 this signaling pathway is a RhoA and ROCK dependent pathway.
306 To confirm that these cellular responses can also be recapitulated by a physiological
307 PAR4 agonist, we tested the ability of thrombin to elicit similar cell shape changes. Since
308 thrombin can also activate PAR1 which is endogenously expressed in HEK-293 cells we
309 conducted these experiments in PAR1 knockout HEK-293 cells (PAR1-KO-HEK) (Mihara
310 *et al.*, 2016) stably expressing PAR4-YFP (PAR1-KO-HEK-PAR4-YFP). PAR1-KO-HEK-
311 PAR4-YFP cells were treated with 3 U/ml thrombin and visualized by confocal
312 microscopy. Treatment of cells with thrombin caused cell shape changes similar to what
313 was observed in HEK-293-PAR4-YFP cells treated with AYPGKF-NH_2 (Fig. 7A). PAR1-
314 KO-HEK-PAR4-YFP cells were then treated with blebbistatin prior to thrombin
315 stimulation (Fig. 7B). Blebbistatin significantly reduced the number of PAR1-KO-HEK-
316 PAR4-YFP cells displaying membrane blebs from 68.3% +/- 4.6 to 11.67% +/- 5.78 (Fig.
317 7D). Finally, PAR1-KO-HEK-PAR4-YFP cells were treated with GSK269962 prior to
318 stimulation with thrombin (Fig. 7C). GSK269962 (100 nM) significantly reduced the
319 number of cells that displayed blebbing in response to thrombin stimulation (Fig. 7D).
320 Together these data indicates that cell blebbing is triggered not only by the synthetic PAR4
321 activating peptide AYPGKF-NH_2, but also by one of the endogenous activators of PAR4,

322 thrombin, in a PAR1 null background. Cell shape changes mediated by thrombin activation
323 of PAR4 are also RhoA- and ROCK-dependent.
324
325 **PAR4 mediated cell shape change is β-arrestin dependent**
326 Since the non-blebbing dRS-PAR4-YFP expressing cells are also deficient in β-
327 arrestin recruitment (Ramachandran *et al.*, 2017), we next examined the contribution of β-
328 arrestin-mediated signaling in PAR4 dependent cell membrane blebbing. To elucidate a
329 role for β-arrestins in PAR4 mediated cell shape change, a β-arrestin-1 and -2 double knock
330 out cell line (β-arr1/2-KO-HEK-293) was created using CRISPR/Cas9 targeting. β-arr1/2-
331 KO-HEK-293 cells transiently expressing PAR4-YFP (β-arr1/2-KO-HEK-293-PAR4-YFP)
332 were treated with 30 μM AYPGKF-NH_2 and visualized by confocal microscopy. A
333 significant reduction in the number of blebbing β-arr1/2-KO-HEK-293-PAR4-YFP
334 (46%+/-8.2) was observed when compared to control HEK-293 cells transiently expressing
335 PAR4-YFP (80.8%+/- 6.1)(Fig. 8A-C).
336 Since recent reports have questioned whether β-arrestin mediated signaling can
337 occur in the absence of G-protein activation (Grundmann *et al.*, 2018) we sought to
338 understand this requirement in the context of PAR4 signaling. Even though $G\alpha_{q/11}$ and $G\alpha_i$
339 recruitment was not implicated in PAR4 dependent membrane blebbing, we nevertheless
340 examined the effect of blocking these pathways on β-arrestin-1/-2 recruitment to PAR4. To
341 this end we blocked $G\alpha_{q/11}$ with the inhibitor YM-254890 (100 nM) and blocked $G\alpha_i$ with
342 pertussis toxin (100 nM) and examined their ability to disrupt β-arrestin recruitment to
343 PAR4-YFP. We employed a BRET assay to monitor interaction between PAR4-YFP and
344 β-arrestin-1-Rluc or β-arrestin 2-Rluc in response to 30, 100 and 300 μM AYPGKF-NH_2.
345 Treatment of cells with YM-254890 did not significantly reduce recruitment of β-arrestin 1
346 or β-arrestin 2 recruitment to PAR4 at 30 μM or 100 μM concentrations of AYPGKF-NH_2
347 but did significanctly reduce recruitment of both β-arrestin-1 and -2 at the 300 μM
348 AYPGKF-NH_2 (Fig. 8D) treatment condition. Treatment of cells with pertussis toxin had
349 no effect on β-arrestin recruitment at any of the concentration tested (Fig. 8E).
350 Finally, we tested a role for Gβγ signaling in PAR4-mediated cell shape change
351 using the Gβγ inhibitor gallein (10 μM). HEK-293 cells stably expressing PAR4-YFP were
352 incubated with gallein or DMSO vehicle control prior to treatment with 30 μM AYPGKF-
353 NH_2. Cells treated with gallein did not show a significant reduction in membrane blebbing
354 compared to DMSO treated cells, 61.75% +/- 4.5 and 85.28% +/- 5.2 (Fig. 9A-C). Cells
355 expressing PAR4-YFP and either β-arrestin-1-Rluc or β-arrestin-2-Rluc incubated with
356 gallein prior to treatment with AYPGKF-NH_2 at 30, 100 and 300 μM also retained their
357 ability to recruit β-arrestin-1 and -2 at all concentrations of AYPGKF-NH_2 (Fig. 9D).
358 Taken together these data show that PAR4-mediated cell shape changes is independent of
359 $G\alpha_{q/11}$, $G\alpha_i$ and Gβγ. Further inhibition of $G\alpha_i$ and Gβγ individually does not impede β-
360 arrestin recruitment to PAR4, while $G\alpha_{q/11}$ inhibition partially reduces β-arrestin
361 recruitment to PAR4.
362
363 **PAR4 activation in rat primary aortic vascular smooth muscle cells leads to cell shape**
364 **changes.**
365 In order to examine whether PAR4 activation triggered cell blebbing in cells that
366 endogenously express PAR4, we turned to the rat vascular smooth muscle cells. Vascular

367 smooth muscle cells are reported to express PAR4 (Bretschneider *et al.*, 2001; Dangwal *et*
368 *al.*, 2011) and in our hands rat aortic smooth muscle cells from both WKY and SHR rats (a
369 kind gift from Dr. Robert Gros) expressed PAR4 (Fig. 10I). We labelled the smooth
370 muscle cell membrane with cell mask (ThermoFisher) and stimulated with 30 μM
371 AYPGKF-NH_2. Both WKY and SHR VSMC displayed cell shape changes resembling
372 membrane blebs in response to PAR4 agonist treatment (Fig 10A, E). In order to establish
373 whether the signaling mechanism for these cell shape changes was the same in both VSMC
374 and HEK-293 cells, we pretreated VSMC with blebbistatin and the ROCK inhibitor
375 GSK269962 prior to activating PAR4 with 30 μM AYPGKF-NH_2. 67.25 +/- 6.6% of
376 WKY cells display cell shape changes in response to PAR4 agonist, (Fig. 10A), which was
377 significantly reduced with treatment blebbistatin (9.0 +/- 3.1%) and with treatment with
378 GSK269962 (6.5 +/- 0.28%) (Fig. 10B-D). Consistent with these findings, 65.75 +/- 5.4%
379 of SHR cells also displayed blebbing following PAR4 activation and these responses were
380 significantly reduced with blebbistatin (14.5 +/- 1.9%) and with GSK269962, (15.5 +/-
381 3.1%) treatment (Fig. 10F-H). These data indicate that endogenous PAR4 activation elicits
382 membrane blebbing in VSMC that is ROCK dependent in keeping with our findings in the
383 HEK-293 cells exogenously expressing PAR4.
384
385 **PAR4 mediated β-arrestin recruitment influences gene transcription.**
386 β-arrestins are scaffold proteins that couple GPCRs to multiple signalling cascades
387 in a manner that is differential to heterotrimeric G-protein coupling (Laporte and Scott,
388 2019). Since PAR4-mediated membrane blebbing is β-arrestin-dependent, we sought to
389 take a complementary approach to explore PAR4-mediated β-arrestin-dependent pathways.
390 In order to do this, we compared the transcriptomes of HEK-293 and β-arr1/2-KO-HEK
391 cells activated with 30 μM AYPGKF-NH_2 for 3 hours as well as the transcriptomes of
392 untreated HEK-293 and β-arr1/2-KO-HEK cells transiently expressing PAR4-YFP.
393 Principal component analysis and hierarchical clustering of gene expression profiles shows
394 clear clustering of HEK-293 samples as well as treated and untreated β-arr1/2-KO-HEK
395 samples (Fig. S1A-D). Differential expression analysis between the HEK-293 cells and β-
396 arr1/2-KO-HEK cells yielded 2,764 and 3,155 significantly differentially expressed genes
397 (P_{adj} <0.05 and Fold-Change>2) between the HEK-293 and β-arr1/2-KO-HEK samples in
398 untreated and treated conditions, respectively. A total of 1,313 differentially expressed
399 genes were shared between the untreated and treated conditions (Fig. 11). Of note, even
400 though we see a depletion of β-arrestin protein in our β-arr1/2-KO-HEK cell line, we do
401 not see down regulation of β-arrestin-1 or -2 transcripts in the RNA seq profile. Gene
402 ontology (GO) enrichment analysis of the significantly upregulated genes in samples
403 treated with 30 μM AYPGKF-NH_2 (N=1506) revealed biological process terms related to
404 cell-cell adhesion, and G-protein coupled receptor signaling pathway which are consistent
405 with our finding of membrane blebbing triggered by PAR4 activation. (Table 1).
406 Additionally, GO terms relating to known functions of PAR4 including neuron-neuron
407 synaptic transmission, blood coagulation, blood circulation, and sensory perception were
408 also found to be enriched in upregulated genes (Table 1). GO analysis of the downregulated
409 genes (Treated only: N=336) revealed biological process terms related to intracellular
410 signal transduction. (Table 2). Taken together, these results suggest that β-arrestin-1/-2 are
411 important regulators of signaling and gene transcription following PAR4 activation. Genes

412 upregulated relating to cell-cell adhesion and GPCR signaling are consistent with our
413 finding of β-arrestin-dependent membrane blebbing following PAR4 activation.
414
415 **Discussion**
416 We have demonstrated that activation of PAR4 with thrombin or the synthetic
417 peptide AYPGKF-NH_2 causes a rapid cell shape change response in PAR4 transfected
418 HEK-293 cells or in vascular smooth muscle cells that endogenously express PAR4. Cell
419 shape changes are pharmacologically inhibited by blebbistatin and are consistent with
420 membrane bleb formation. We observed membrane blebs that formed within 2-5 minutes of
421 agonist treatment and lasted for upto 30 minutes. Membrane blebbing could be
422 pharmacologically inhibited by the ROCK inhibitor GSK269962 or through CRISPR/Cas9
423 mediated knockout of RhoA. CRISPR/Cas9 knockout of β-arrestin-1 and -2 partially
424 abolished PAR4-dependent mebrane blebbing. We further found PAR4-dependent
425 membrane bleb formation to be independent of $G\alpha_{q/11}$, $G\alpha_{i,}$ $G\beta\gamma$, and PKC. Overall, our
426 data suggest that RhoA-dependent membrane blebbing occurs downstream of PAR4
427 activation and β-arrestin recruitment.
428 Non-apoptotic cell membrane blebbing plays an important role in various
429 physiological and pathologlical processes. Various stimuli have been reported to trigger
430 bleb formation leading to cellular responses including enhanced cell motility, invasion, cell
431 locomotion, and regulation of cell polarity in embryonic development (Charras and Paluch,
432 2008; Fackler and Grosse, 2008; Ikenouchi and Aoki, 2016). Blebbing is also an important
433 regulator of wound healing, immune cell maturation, and inflammation. In this context, the
434 PAR family of GPCRs is well established as critical regulators of the innate immune
435 response to injury and infection. PARs also elicit cellular responses that allow coagulation
436 cascade enzymes such as thrombin and other serine proteinases to regulate various cellular
437 functions. PAR1 and PAR4 serve as the receptors for thrombin on human platelets, though
438 these receptors regulate different aspects of platelet activation (Coughlin, 1999; Kahn *et al.*,
439 1999; Ma *et al.*, 2005; Holinstat *et al.*, 2006; Voss *et al.*, 2007). PAR4 is described as the
440 low affinity thrombin receptor on human platelets. This lower affinity stems from the lack
441 of a hirudin like binding site for thrombin on PAR4, that is present on PAR1. In platelets,
442 PAR4 activation typically requires a much higher concentration of thrombin to be present
443 and PAR4 activation typically results in more sustained calcium signaling compared to
444 PAR1 dependent signaling (Covic *et al.*, 2000; Shapiro *et al.*, 2000).
445 Both PAR1 and PAR4 activation triggers platelet aggregation, with PAR4 signaling
446 critical for full platelet spreading and formation of stable aggregates. In rodents PAR4
447 serves as the sole thrombin receptor in platelets (Sambrano *et al.*, 2001). It has been
448 previously shown in $G\alpha_{q/11}$ knock out mice, that a thrombin activated $G\alpha_{q/11}$-mediated
449 calcium response is necessary for platelet aggregation (Offermanns *et al.*, 1997). However,
450 platelets from the mouse $G\alpha_{q/11}$ knockout retained the ability to change shape in response to
451 thrombin stimulation. Similar findings were reported in platelets treated with a small
452 molecule $G\alpha_{q/11}$ antagonist UBO-QIC showing that platelet aggregation was inhibited
453 without affecting shape change responses (Inamdar *et al.*, 2015). Consistent with these
454 findings, we have observed a cell shape change specific to PAR4 activation that is $G_{q/11}$-
455 independent and a RhoA-mediated phenomenon. Recent evidence suggests that PAR4
456 plays an important role in promoting platelet granule release and platelet-leukocyte
457 interactions (Rigg *et al.*, 2019), responses which also rely on a RhoA-mediated cytoskeletal

458 rearrangement (Moers *et al.*, 2003; Aslan and Mccarty, 2013). These findings raise the
459 interesting possibility that different signaling pathways may underlie PAR4 regulation of
460 distinct aspects of platelet activation and further study is required to fully elucidate the role
461 of different signaling cascades in mediating PAR4 responses in platelets. Our studies
462 suggest that in HEK cells the $G\alpha_{q/11}$ coupled pathway and the RhoA pathway, which in this
463 instance is likely downstream of $G\alpha_{12/13}$ coupling, can act independently and therefore may
464 be independent targets for pharmacological manipulation.
465 PAR4 expression has also been reported in other cell types involved in the response
466 to injury including endothelial cells and smooth muscle cells (Bretschneider *et al.*, 2001;
467 Hamilton *et al.*, 2001; Fujiwara *et al.*, 2005; Ritchie *et al.*, 2007). Here we demonstrate that
468 agonist stimulation of endogenous PAR4 in vascular smooth muscle cells leads to
469 membrane blebbing. This finding is consistent with a previous study which showed that
470 another GPCR AT1R mediates membrane blebbing by a RhoA-dependent mechanism in a
471 vascular smooth muscle cell line (Godin and Ferguson, 2010). RhoA is well established as
472 a mediator of changes in the plasma membrane actin cytoskeleton and in regulating GPCR
473 mediated cell shape change (Barnes *et al.*, 2005; Godin and Ferguson, 2010; Aoki *et al.*,
474 2016). Our findings add PAR4-dependent signaling to the cell surface signaling molecules
475 that can trigger this pathway.
476 β-arrestins are now well established as important molecular scaffolds linking
477 GPCRs to not only molecular endocytic partners to facilitate receptor endocytosis, but also
478 to second messenger signal cascades (Ferguson, 2001; Magalhaes *et al.*, 2012). For
479 example β-arrestins link GPCRs to p44/42 MAP kinase signalling from the endosome
480 (Luttrell *et al.*, 2001; Luttrell and Lefkowitz, 2002). PAR4 couples to both β-arrestin-1 and
481 β-arrestin-2 and PAR4-mediated phosphorylation of AKT in platelets is β-arrestin-2-
482 dependent (Li *et al.*, 2011). We explored β-arrestin-1/-2-dependent PAR4 signaling by
483 using RNA sequencing analysis in HEK cells and β-arrestin knock out HEK cells treated or
484 not with the PAR4 specific agonist peptide AYPGKF-NH_2. Our data shows that β-arrestins
485 can regulate PAR4-dependent gene transcription. Consistent with our finding that PAR4
486 mediates membrane bleb formation, we see an upregulation of gene ontology terms in cell-
487 cell adhesion, blood coagulation and blood circulation. It is well established that PAR4
488 activation regulates platelet response and links to gene ontology terms related to blood
489 coagulation are perhaps unsurprising but uncover an important link to β-arrestin in these
490 processes. Our RNAseq analysis uncovered a number of other additional signaling
491 pathways that could be linked to PAR4 and β-arrestin such as neuron-neuron synaptic
492 transmission (GO:0007270), natural killer cell activation (GO:0030101) and sensory
493 perception (GO:0007600). PAR4 expression has been reported in various neuronal and
494 immune cells and these data provide impetus to further examine the roles of PAR4 in these
495 cells (Henrich-Noack *et al.*, 2006; Russell *et al.*, 2009; Peng *et al.*, 2019). More broadly
496 were also interested in understanding if PAR4 signaling to β-arrestin could proceed
497 independently of G-protein coupling. Blocking $G\alpha_{q/11}$ partially inhibited β-arrestin
498 recruitment to PAR4 while blocking of $G\alpha_i$- or βγ-mediated signaling had no effect. It
499 however remains to be determined whether β-arrestin recruitment dependent signaling
500 downstream of PAR4 is truly independent of G-protein coupling or occurs following
501 $G\alpha_{12/13}$ activation.

502 In conclusion, we have uncovered a PAR4-mediated cellular response that is
503 independent of $G\alpha_{q/11}$ coupling and occurs downstream of RhoA activation and β-arrestin
504 signaling. These data provide further evidence for pathway selective signaling responses
505 through PAR4 and guide future development of PAR4 targeting strategies.

506 **Figure Legends:**
507
508 **Figure 1. Activation PAR4 mediates a cell shape change response.** Representative
509 confocal micrographs, showing HEK-293 cell stably expressing PAR4-YFP (A, B) Cells
510 were treated with 30 μM AYPGKF-NH_2 for 2 minutes prior to imaging. Size bars are 20
511 μm, arrows show cell shape change. HEK-293 cells stably expressing PAR4-YFP (C-E)
512 were incubated in either DMSO (C) or 10 μM blebbistatin (B) for 15 minutes prior to a 2-
513 minute treatment with 30 μM AYPGKF-NH_2 followed by confocal microscopy. Arrows
514 show bleb formation, size bars are 20 μm. (E) graph shows mean +/- SEM, n=4, asterisk
515 shows significantly different, Mann-Whitney, $p<0.05$.
516
517 **Figure 2. Activation PAR4 mediates a cell shape change response is dependent on an 8**
518 **amino acid sequence.**
519 HEK 293 transiently expressing dRS-PAR4-YFP (A-C) were treated with 30 μM
520 AYPGKF-NH_2 for 2 minutes prior to imaging and scored for cell shape change or no
521 change, graph shows mean +/- SEM, size bars are 20 μm, asterisks indicates statistically
522 significant, t-test, N=3, $p<0.005$.
523
524 **Figure 3. PAR4-mediated cell shape change is $G\alpha_{q/11}$-independent.** HEK-293 cells
525 transiently expressing PAR4-mCherry (not shown) with PKCβ1-GFP, were treated with
526 DMSO followed by stimulation with 30 μM AYPGKF-NH_2 (A-C) or with 100 nM
527 YM254890 for 20 minutes followed by stimulation with 30 μM AYPGKF-NH_2 (D-F).
528 Arrows show bleb formation, size bars are 20 μm. Graph shows mean +/- SEM, n=3, not
529 significantly different, t-test (G).
530
531 **Figure 4. PAR4-mediated cell shape change is PKC-independent.** HEK-293 cells
532 transiently expressing either PAR4-mCherry (not shown) (A, B) or dRS-PAR4-mCherry
533 (not shown) (C, D) with PKCβ1-GFP, were treated with 30 μM AYPGKF-NH_2 and imaged
534 by confocal microscopy, size bars are 20 μm. HEK-293 cells stably expressing PAR4-YFP
535 were incubated with DMSO (E) or with 100 nM GO6983 for 15 minutes (F) prior to 2 a
536 minute stimulation with 30 μM AYPGKF-NH_2 and subsequent imaging by confocal
537 microscopy. Cells were scored for blebbing or non-blebbing, graph shows mean +/- SEM,
538 n=4, not significantly different, t-test (G).
539
540 **Figure 5. PAR4-mediated cell shape change is $G\alpha_i$-independent.** HEK-293 cells stably
541 expressing PAR4-YFP were incubated in either DMSO (A) or 100 nM PTX (B) for 18
542 hours prior to 30 μM AYPGKF-NH_2 treatment for 2 minutes and confocal imaging.
543 Arrows show bleb formation, size bars are 20 μm. Graphs shows mean +/- SEM, n=3, not
544 significantly different, Mann-Whitney (C).
545
546 **Figure 6. PAR4-mediated cell shape change is RhoA- and ROCK-dependent.** HEK-
547 293 cells stably expressing PAR4-YFP were incubated in either DMSO (A) or 100 nM
548 GSK269962 for 1 hour (B) prior to a 2-minute treatment with 30 μM AYPGKF-NH_2
549 followed by confocal microscopy. Arrows show bleb formation, size bars are 20 μm. (C)
550 graph shows mean +/- SEM, n=4, asterisk shows significantly different, Mann-Whitney,

551 p<0.05. HEK-293 cells and RhoA-KO HEK transiently expressing PAR4-YFP were
552 stimulated with 30 μM AYPGKF-NH_2 for 2 minutes prior to confocal imaging (D, E). (F)
553 Graph shows mean +/- SEM, n=4, asterisk shows significantly different, Mann-Whitney,
554 p<0.05.
555
556 **Figure 7. Thrombin-induced PAR4-mediated cell shape change is ROCK-dependent.**
557 PAR1 KO-PAR4-YFP-HEK 293 cells were incubated in either DMSO (A) or 10 μM
558 blebbistatin for 15 minutes (B) or 100 nM GSK269962 for 1 hour (C) prior to a 2-minute
559 treatment with 30 μM AYPGKF-NH_2 followed by confocal microscopy. Arrows show bleb
560 formation, size bars are 20 μm. Graph shows mean +/- SEM, n=4, asterisk shows
561 significantly different, Mann-Whitney, p<0.05 (D).
562
563 **Figure 8. PAR4-mediated cell shape change is β-arrestin-dependent.** HEK-293 cells
564 (A) or β-arr1/2-KO-HEK transiently expressing PAR4-YFP (B) were stimulated in 30 μM
565 AYPGKF-NH_2 for 2 minutes prior to confocal imaging. Arrows show bleb formation, size
566 bars are 20 μm. (C) Graph shows mean +/- SEM, n=3, asterisk shows significantly
567 different, t-test, P<0.05). HEK-293 cells transiently expressing PAR4-YFP with either β-
568 arrestin 1-Rluc or β-arrestin 2-Rluc were incubated in DMSO or 100 nM YM254890 (D) or
569 100 nM PTX for 18 hours (E) for 20 minutes prior to testing in the BRET assay. Graph
570 shows mean +/- SEM, n=4, asterisk shows significantly different, 2-way ANOVA.
571
572 **Figure 9. PAR4-mediated cell shape change is $G_{\beta\gamma}$-independent.** HEK-293 cells stably
573 expressing PAR4-YFP were incubated in either DMSO (A) or 10 μM gallein for 20
574 minutes prior to 30 μM AYPGKF-NH_2 for 2 minutes and confocal imaging. Arrows show
575 bleb formation, size bars are 20 μm. Graphs shows mean +/- SEM, n=4, not significantly
576 different, Mann-Whitney (C). HEK-293 cells transiently expressing PAR4-YFP with either
577 β-arrestin 1-Rluc or β-arrestin 2-Rluc were incubated in DMSO or with 10 μM gallein for
578 20 minutes (H) prior to testing in the BRET assay. Graph shows, mean +/- SEM, n=4, not
579 significantly different 2-way ANOVA.
580
581 **Figure 10. PAR4 mediates membrane blebs in vascular smooth muscle cells.** Primary
582 cultured vascular smooth muscle cells derived from Wistar Kyoto (WKY) (A-D) or from
583 spontaneously hypertensive (SHR) (E-H) rats were pre-incubated for 10 minutes in cell
584 mask to stain the plasma membrane, cells were then treated with 30 mM AYPGFK-$NH_2$and
585 imaged by confocal microscopy. WKY cells and SHR cells were pre-incubated with
586 blebbistatin or with GSK269962 prior to stimulation with AYPGFK-NH_2 (B, C, F, G),
587 arrows show bleb formation, size bars are 20 μm. Images were scored for blebbing or
588 non-blebbing (D and H), graph shows mean +/- SEM, n=4, asterisk shows significantly
589 different, ANOVA, p<0.001.
590
591 **Table 1: Differential PAR4-mediated gene regulation in β-arrestin-1/-2 knock out**
592 **cells.**
593 Gene ontology (GO) biological process terms for genes upregulated (A) and downregulated
594 (B) genes in β-arr-1/-2-KO-HEK cells transiently expressing PAR4-YFP treated with 30
595 μM AYPGKF-NH_2 for 3 hours compared to HEK-293 cells under the same conditions. Top

596 ten significant terms ($p<0.05$) where the highest enrichment for biological process are
597 presented. Terms related to the membrane blebbing phenotype are in bold and terms related
598 to known functions of PAR4 are italicized.
599
600 **Supplementary Figure 1. CRISPR/Cas9 knock out of of β-arrestin-1/-2 and RhoA in**
601 **HEK 293 cells.**
602 HEK 293 cells were transiently transfected with either guide RNA specific to β-arrestin1
603 and β-arrestin 2, or four guide RNAs specific to RhoA. Cells expressing pSpCas9(BB)-
604 2A-GFP encoding guide RNAs were selected for using FACS Aria cell sorter and
605 subsequently knockout was determined by western blot.
606
607 **Supplementary Figure 2. Knockout of β-arrestin-1/-2 results in differentially**
608 **expressed genes. (A)**Principal component analysis biplot showing the first two principal
609 components (PCs) that account for most of the variance between samples. **(B)** Venn
610 diagram showing overlap of differentially expressed genes ($P_{adj}<0.05$ and Fold-Change>2)
611 in β-arrestin 1/2 knockout cells treated with PAR4 agonist (Treated) or with vehicle
612 (Untreated) when compared to similarly treated HEK 293 cells. **(C & D)** Volcano plots
613 showing significantly differentially expressed genes between β-arrestin 1/2 knockout cells
614 and HEK293 cells when treated with vehicle **(C)** or 30 μM AYPGKF-NH_2 **(D)**. Of the
615 differentially expressed genes, 666 were downregulated and unique to untreated cells, 336
616 were downregulated and unique to treated cells, and 636 were found to be downregulated in
617 both conditions. Additionally, 785 genes were upregulated and unique to untreated cells,
618 1506 were upregulated and unique to treated cells, and 667 were found to be upregulated in
619 both conditions.
620

621 **References:**
622

623 Anders S, Pyl PT, and Huber W (2015) HTSeq--a Python framework to work with high-
624 throughput sequencing data. *Bioinforma Oxf Engl* **31**:166–169.

625 Anthony DF, Sin YY, Vadrevu S, Advant N, Day JP, Byrne AM, Lynch MJ, Milligan G,
626 Houslay MD, and Baillie GS (2011) β-Arrestin 1 inhibits the GTPase-activating
627 protein function of ARHGAP21, promoting activation of RhoA following
628 angiotensin II type 1A receptor stimulation. *Mol Cell Biol* **31**:1066–1075.

629 Aoki K, Maeda F, Nagasako T, Mochizuki Y, Uchida S, and Ikenouchi J (2016) A RhoA
630 and Rnd3 cycle regulates actin reassembly during membrane blebbing. *Proc Natl*
631 *Acad Sci U S A* **113**:E1863-1871.

632 Aslan JE, and Mccarty OJT (2013) Rho GTPases in platelet function. *J Thromb Haemost*
633 **11**:35–46.

634 Barnes WG, Reiter E, Violin JD, Ren XR, Milligan G, and Lefkowitz RJ (2005) beta-
635 Arrestin 1 and Galphaq/11 coordinately activate RhoA and stress fiber formation
636 following receptor stimulation. *J Biol Chem* **280**:8041–8050.

637 Bretschneider E, Kaufmann R, Braun M, Nowak G, Glusa E, and Schror K (2001)
638 Evidence for functionally active protease-activated receptor-4 (PAR-4) in human
639 vascular smooth muscle cells. *Br J Pharmacol* **132**:1441–1446.

640 Charras G, and Paluch E (2008) Blebs lead the way: how to migrate without lamellipodia.
641 *Nat Rev Mol Cell Biol* **9**:730–736.

642 CHARRAS GT (2008) A short history of blebbing. *J Microsc* **231**:466–478.

643 Charras GT, Coughlin M, Mitchison TJ, and Mahadevan L (2008) Life and Times of a
644 Cellular Bleb. *Biophys J* **94**:1836–1853.

645 Chen P, Douglas SD, Meshki J, and Tuluc F (2012) Neurokinin 1 receptor mediates
646 membrane blebbing and sheer stress-induced microparticle formation in HEK293
647 cells. *PloS One* **7**:e45322.

648 Cheung A, Dantzig JA, Hollingworth S, Baylor SM, Goldman YE, Mitchison TJ, and
649 Straight AF (2002) A small-molecule inhibitor of skeletal muscle myosin II. *Nat*
650 *Cell Biol* **4**:83–88.

651 Coughlin SR (1999) How the protease thrombin talks to cells. *Proc Natl Acad Sci U S A*
652 **96**:11023–11027.

653 Covic L, Gresser AL, and Kuliopulos A (2000) Biphasic kinetics of activation and
654 signaling for PAR1 and PAR4 thrombin receptors in platelets. *Biochemistry*
655 **39**:5458–5467.

656 Dale LB, Babwah AV, Bhattacharya M, Kelvin DJ, and Ferguson SS (2001) Spatial-
657 temporal patterning of metabotropic glutamate receptor-mediated inositol 1,4,5-
658 triphosphate, calcium, and protein kinase C oscillations: protein kinase C-dependent
659 receptor phosphorylation is not required. *J Biol Chem* **276**:35900–35908.

660 Dangwal S, Rauch BH, Gensch T, Dai L, Bretschneider E, Vogelaar CF, Schrör K, and
661 Rosenkranz AC (2011) High glucose enhances thrombin responses via protease-
662 activated receptor-4 in human vascular smooth muscle cells. *Arterioscler Thromb*
663 *Vasc Biol* **31**:624–633.

664 Dobin A, Davis CA, Schlesinger F, Drenkow J, Zaleski C, Jha S, Batut P, Chaisson M, and
665 Gingeras TR (2013) STAR: ultrafast universal RNA-seq aligner. *Bioinformatics*
666 **29**:15–21.

667 Exton JH (1996) Regulation of phosphoinositide phospholipases by hormones,
668 neurotransmitters, and other agonists linked to G proteins. *Annu Rev Pharmacol*
669 *Toxicol* **36**:481–509.

670 Fackler OT, and Grosse R (2008) Cell motility through plasma membrane blebbing. *J Cell*
671 *Biol* **181**:879–884.

672 Ferguson SS (2001) Evolving concepts in G protein-coupled receptor endocytosis: the role
673 in receptor desensitization and signaling. *Pharmacol Rev* **53**:1–24.

674 Ferguson SSG, and Caron MG (2004) Green Fluorescent Protein-Tagged β-Arrestin
675 Translocation as a Measure of G Protein-Coupled Receptor Activation, in *G Protein*
676 *Signaling: Methods and Protocols* (Smrcka AV ed) pp 121–126, Humana Press,
677 Totowa, NJ.

678 Fujiwara M, Jin E, Ghazizadeh M, and Kawanami O (2005) Activation of PAR4 induces a
679 distinct actin fiber formation via p38 MAPK in human lung endothelial cells. *J*
680 *Histochem Cytochem* **53**:1121–1129.

681 Godin CM, and Ferguson SSG (2010) The angiotensin II type 1 receptor induces
682 membrane blebbing by coupling to Rho A, Rho kinase, and myosin light chain
683 kinase. *Mol Pharmacol* **77**:903–911.

684 Gong X, Didan Y, Lock JG, and Strömblad S (2018) KIF13A-regulated RhoB plasma
685 membrane localization governs membrane blebbing and blebby amoeboid cell
686 migration. *EMBO J* **37**.

687 Gros Robert, Ding Qingming, Chorazyczewski Jozef, Pickering J. Geoffrey, Limbird Lee
688 E., and Feldman Ross D. (2006) Adenylyl Cyclase Isoform–Selective Regulation of
689 Vascular Smooth Muscle Proliferation and Cytoskeletal Reorganization. *Circ Res*
690 **99**:845–852.

691 Grundmann M, Merten N, Malfacini D, Inoue Asuka, Preis P, Simon K, Rüttiger N, Ziegler
692 N, Benkel T, Schmitt NK, Ishida S, Müller I, Reher R, Kawakami K, Inoue Ayumi,

693 Rick U, Kühl T, Imhof D, Aoki J, König GM, Hoffmann C, Gomeza J, Wess J, and
694 Kostenis E (2018) Lack of beta-arrestin signaling in the absence of active G
695 proteins. *Nat Commun* **9**:341.

696 Gschwendt M, Dieterich S, Rennecke J, Kittstein W, Mueller HJ, and Johannes FJ (1996)
697 Inhibition of protein kinase C mu by various inhibitors. Differentiation from protein
698 kinase c isoenzymes. *FEBS Lett* **392**:77–80.

699 Hagmann J, Burger MM, and Dagan D (1999) Regulation of plasma membrane blebbing by
700 the cytoskeleton. *J Cell Biochem* **73**:488–499.

701 Hamilton JR, Frauman AG, and Cocks TM (2001) Increased expression of protease-
702 activated receptor-2 (PAR2) and PAR4 in human coronary artery by inflammatory
703 stimuli unveils endothelium-dependent relaxations to PAR2 and PAR4 agonists.
704 *Circ Res* **89**:92–98.

705 Henrich-Noack P, Riek-Burchardt M, Baldauf K, Reiser G, and Reymann KG (2006) Focal
706 ischemia induces expression of protease-activated receptor1 (PAR1) and PAR3 on
707 microglia and enhances PAR4 labeling in the penumbra. *Brain Res* **1070**:232–241.

708 Holinstat M, Voss B, Bilodeau ML, McLaughlin JN, Cleator J, and Hamm HE (2006)
709 PAR4, but not PAR1, signals human platelet aggregation via Ca2+ mobilization and
710 synergistic P2Y12 receptor activation. *J Biol Chem* **281**:26665–26674.

711 Ikenouchi J, and Aoki K (2016) Membrane bleb: A seesaw game of two small GTPases. -
712 PubMed - NCBI. *Small GTPases* **8**:85–89.

713 Inamdar V, Patel A, Manne BK, Dangelmaier C, and Kunapuli SP (2015) Characterization
714 of UBO-QIC as a Gαq inhibitor in platelets. *Platelets* **26**:771–778.

715 Kahn ML, Nakanishi-Matsui M, Shapiro MJ, Ishihara H, and Coughlin SR (1999)
716 Protease-activated receptors 1 and 4 mediate activation of human platelets by
717 thrombin. *J Clin Invest* **103**:879–887.

718 Kim S, Jin J, and Kunapuli SP (2006) Relative contribution of G-protein-coupled pathways
719 to protease-activated receptor-mediated Akt phosphorylation in platelets. *Blood*
720 **107**:947–954.

721 Kovács M, Tóth J, Hetényi C, Málnási-Csizmadia A, and Sellers JR (2004) Mechanism of
722 blebbistatin inhibition of myosin II. *J Biol Chem* **279**:35557–35563.

723 Laporte SA, and Scott MGH (2019) β-Arrestins: Multitask Scaffolds Orchestrating the
724 Where and When in Cell Signalling. *Methods Mol Biol Clifton NJ* **1957**:9–55.

725 Laser-Azogui A, Diamant-Levi T, Israeli S, Roytman Y, and Tsarfaty I (2014) Met-induced
726 membrane blebbing leads to amoeboid cell motility and invasion. *Oncogene*
727 **33**:1788–1798.

728 Lawrenson ID, Wimmer-Kleikamp SH, Lock P, Schoenwaelder SM, Down M, Boyd AW,
729 Alewood PF, and Lackmann M (2002) Ephrin-A5 induces rounding, blebbing and
730 de-adhesion of EphA3-expressing 293T and melanoma cells by CrkII and Rho-
731 mediated signalling. *J Cell Sci* **115**:1059–1072.

732 Li D, D'Angelo L, Chavez M, and Woulfe DS (2011) Arrestin-2 Differentially Regulates
733 PAR4 and ADP Receptor Signaling in Platelets. *J Biol Chem* **286**:3805–3814.

734 Love MI, Huber W, and Anders S (2014) Moderated estimation of fold change and
735 dispersion for RNA-seq data with DESeq2. *Genome Biol* **15**:550.

736 Luttrell LM, and Lefkowitz RJ (2002) The role of beta-arrestins in the termination and
737 transduction of G-protein-coupled receptor signals. *J Cell Sci* **115**:455–465.

738 Luttrell LM, Roudabush FL, Choy EW, Miller WE, Field ME, Pierce KL, and Lefkowitz
739 RJ (2001) Activation and targeting of extracellular signal-regulated kinases by beta-
740 arrestin scaffolds. *Proc Natl Acad Sci* **98**:2449–2454.

741 Ma L, Perini R, McKnight W, Dicay M, Klein A, Hollenberg MD, and Wallace JL (2005)
742 Proteinase-activated receptors 1 and 4 counter-regulate endostatin and VEGF
743 release from human platelets. *Proc Natl Acad Sci U S A* **102**:216–220.

744 Magalhaes AC, Dunn H, and Ferguson SS (2012) Regulation of GPCR activity, trafficking
745 and localization by GPCR-interacting proteins. *Br J Pharmacol* **165**:1717–1736.

746 Mi H, Huang X, Muruganujan A, Tang H, Mills C, Kang D, and Thomas PD (2017)
747 PANTHER version 11: expanded annotation data from Gene Ontology and
748 Reactome pathways, and data analysis tool enhancements. *Nucleic Acids Res*
749 **45**:D183–D189.

750 Mihara K, Ramachandran R, Saifeddine M, Hansen KK, Renaux B, Polley D, Gibson S,
751 Vanderboor C, and Hollenberg MD (2016) Thrombin-Mediated Direct Activation
752 of Proteinase-Activated Receptor-2: Another Target for Thrombin Signaling. *Mol*
753 *Pharmacol* **89**:606–614.

754 Moers A, Nieswandt B, Massberg S, Wettschureck N, Gruner S, Konrad I, Schulte V,
755 Aktas B, Gratacap MP, Simon MI, Gawaz M, and Offermanns S (2003) G13 is an
756 essential mediator of platelet activation in hemostasis and thrombosis. *Nat Med*
757 **9**:1418–1422.

758 Morrow DA, Braunwald E, Bonaca MP, Ameriso SF, Dalby AJ, Fish MP, Fox KA, Lipka
759 LJ, Liu X, Nicolau JC, Ophuis AJ, Paolasso E, Scirica BM, Spinar J, Theroux P,
760 Wiviott SD, Strony J, and Murphy SA (2012) Vorapaxar in the secondary
761 prevention of atherothrombotic events. *N Engl J Med* **366**:1404–1413.

762 Offermanns S, Toombs CF, Hu Y-H, and Simon MI (1997) Defective platelet activation in
763 Gα q -deficient mice. *Nature* **389**:183.

764 Peng Q, Ratnasothy K, Boardman DA, Jacob J, Tung SL, McCluskey D, Smyth LA,
765 Lechler RI, Dorling A, and Lombardi G (2019) Protease Activated Receptor 4 as a
766 Novel Modulator of Regulatory T Cell Function. *Front Immunol* **10**.

767 Pinner S, and Sahai E (2008) PDK1 regulates cancer cell motility by antagonising
768 inhibition of ROCK1 by RhoE. *Nat Cell Biol* **10**:127–137.

769 Policha A, Daneshtalab N, Chen L, Dale LB, Altier C, Khosravani H, Thomas WG,
770 Zamponi GW, and Ferguson SSG (2006) Role of angiotensin II type 1A receptor
771 phosphorylation, phospholipase D, and extracellular calcium in isoform-specific
772 protein kinase C membrane translocation responses. *J Biol Chem* **281**:26340–26349.

773 Ramachandran R, Mihara K, Mathur M, Rochdi MD, Bouvier M, DeFea K, and Hollenberg
774 MD (2009) Agonist-biased signaling via proteinase activated receptor-2: differential
775 activation of calcium and mitogen-activated protein kinase pathways. *Mol*
776 *Pharmacol* **76**:791–801.

777 Ramachandran R, Mihara K, Thibeault P, Vanderboor CM, Petri B, Saifeddine M, Bouvier
778 M, and Hollenberg MD (2017) Targeting a Proteinase-Activated Receptor 4 (PAR4)
779 Carboxyl Terminal Motif to Regulate Platelet Function. *Mol Pharmacol* **91**:287–
780 295.

781 Ramachandran R, Noorbakhsh F, Defea K, and Hollenberg MD (2012) Targeting
782 proteinase-activated receptors: therapeutic potential and challenges. *Nat Rev Drug*
783 *Discov* **11**:69–86.

784 Rigg RA, Healy LD, Chu TT, Ngo ATP, Mitrugno A, Zilberman-Rudenko J, Aslan JE,
785 Hinds MT, Vecchiarelli LD, Morgan TK, Gruber A, Temple KJ, Lindsley CW,
786 Duvernay MT, Hamm HE, and McCarty OJT (2019) Protease-activated receptor 4
787 activity promotes platelet granule release and platelet-leukocyte interactions.
788 *Platelets* **30**:126–135.

789 Ritchie E, Saka M, Mackenzie C, Drummond R, Wheeler-Jones C, Kanke T, and Plevin R
790 (2007) Cytokine upregulation of proteinase-activated-receptors 2 and 4 expression
791 mediated by p38 MAP kinase and inhibitory kappa B kinase beta in human
792 endothelial cells. *Br J Pharmacol* **150**:1044–1054.

793 Russell FA, Veldhoen VE, Tchitchkan D, and McDougall JJ (2009) Proteinase-activated
794 receptor-4 (PAR4) activation leads to sensitization of rat joint primary afferents via
795 a bradykinin B2 receptor-dependent mechanism. *J Neurophysiol* **103**:155–163.

796 Sah VP, Seasholtz TM, Sagi SA, and Brown JH (2000) The role of Rho in G protein-
797 coupled receptor signal transduction. *Annu Rev Pharmacol Toxicol* **40**:459–489.

798 Sambrano GR, Weiss EJ, Zheng YW, Huang W, and Coughlin SR (2001) Role of thrombin
799 signalling in platelets in haemostasis and thrombosis. *Nature* **413**:74–78.

800 Schmieder R, and Edwards R (2011) Quality control and preprocessing of metagenomic
801 datasets. *Bioinformatics* **27**:863–864.

802 Shapiro MJ, Weiss EJ, Faruqi TR, and Coughlin SR (2000) Protease-activated receptors 1
803 and 4 are shut off with distinct kinetics after activation by thrombin. *J Biol Chem*
804 **275**:25216–25221.

805 Stavenger RA, Cui H, Dowdell SE, Franz RG, Gaitanopoulos DE, Goodman KB, Hilfiker
806 MA, Ivy RL, Leber JD, Marino Joseph P, Oh H-J, Viet AQ, Xu W, Ye G, Zhang D,
807 Zhao Y, Jolivette LJ, Head MS, Semus SF, Elkins PA, Kirkpatrick RB, Dul E,
808 Khandekar SS, Yi T, Jung DK, Wright LL, Smith GK, Behm DJ, Doe CP, Bentley
809 R, Chen ZX, Hu E, and Lee D (2007) Discovery of Aminofurazan-
810 azabenzimidazoles as Inhibitors of Rho-Kinase with High Kinase Selectivity and
811 Antihypertensive Activity. *J Med Chem* **50**:2–5.

812 Straight AF, Cheung A, Limouze J, Chen I, Westwood NJ, Sellers JR, and Mitchison TJ
813 (2003) Dissecting temporal and spatial control of cytokinesis with a myosin II
814 Inhibitor. *Science* **299**:1743–1747.

815 Taniguchi M, Suzumura K, Nagai K, Kawasaki T, Takasaki J, Sekiguchi M, Moritani Y,
816 Saito T, Hayashi K, Fujita S, Tsukamoto S, and Suzuki K (2004) YM-254890
817 analogues, novel cyclic depsipeptides with Gαq/11 inhibitory activity from
818 Chromobacterium sp. QS3666. *Bioorg Med Chem* **12**:3125–3133.

819 Tinevez J-Y, Schulze U, Salbreux G, Roensch J, Joanny J-F, and Paluch E (2009) Role of
820 cortical tension in bleb growth. *Proc Natl Acad Sci U S A* **106**:18581–18586.

821 Voss B, McLaughlin JN, Holinstat M, Zent R, and Hamm HE (2007) PAR1, but not PAR4,
822 activates human platelets through a Gi/o/phosphoinositide-3 kinase signaling axis.
823 *Mol Pharmacol* **71**:1399–1406.

824 Wettschureck N, and Offermanns S (2005) Mammalian G proteins and their cell type
825 specific functions. *Physiol Rev* **85**:1159–1204.

826 Wilson SJ, Ismat FA, Wang Z, Cerra M, Narayan H, Raftis J, Gray TJ, Connell S, Garonzik
827 S, Ma X, Yang J, and Newby DE (2017) PAR4 (Protease-Activated Receptor 4)
828 Antagonism With BMS-986120 Inhibits Human Ex Vivo Thrombus Formation.
829 *Arterioscler Thromb Vasc Biol* ATVBAHA.117.310104.

830 Wong PC, Seiffert D, Bird JE, Watson CA, Bostwick JS, Giancarli M, Allegretto N, Hua J,
831 Harden D, Guay J, Callejo M, Miller MM, Lawrence RM, Banville J, Guy J,
832 Maxwell BD, Priestley ES, Marinier A, Wexler RR, Bouvier M, Gordon DA,
833 Schumacher WA, and Yang J (2017) Blockade of protease-activated receptor-4
834 (PAR4) provides robust antithrombotic activity with low bleeding. *Sci Transl Med*
835 **9**:eaaf5294.

836 Woulfe DS (2005) REVIEW ARTICLES: Platelet G protein-coupled receptors in
837 hemostasis and thrombosis. *J Thromb Haemost* **3**:2193–2200.

838 Xu WF, Andersen H, Whitmore TE, Presnell SR, Yee DP, Ching A, Gilbert T, Davie EW,
839 and Foster DC (1998) Cloning and characterization of human protease-activated
840 receptor 4. *Proc Natl Acad Sci U S A* **95**:6642–6646.

841 Zhang D, LaFortune TA, Krishnamurthy S, Esteva FJ, Cristofanilli M, Liu P, Lucci A,
842 Singh B, Hung M-C, Hortobagyi GN, and Ueno NT (2009) Epidermal growth factor
843 receptor tyrosine kinase inhibitor reverses mesenchymal to epithelial phenotype and
844 inhibits metastasis in inflammatory breast cancer. *Clin Cancer Res Off J Am Assoc*
845 *Cancer Res* **15**:6639–6648.

846

847

Figure 1:

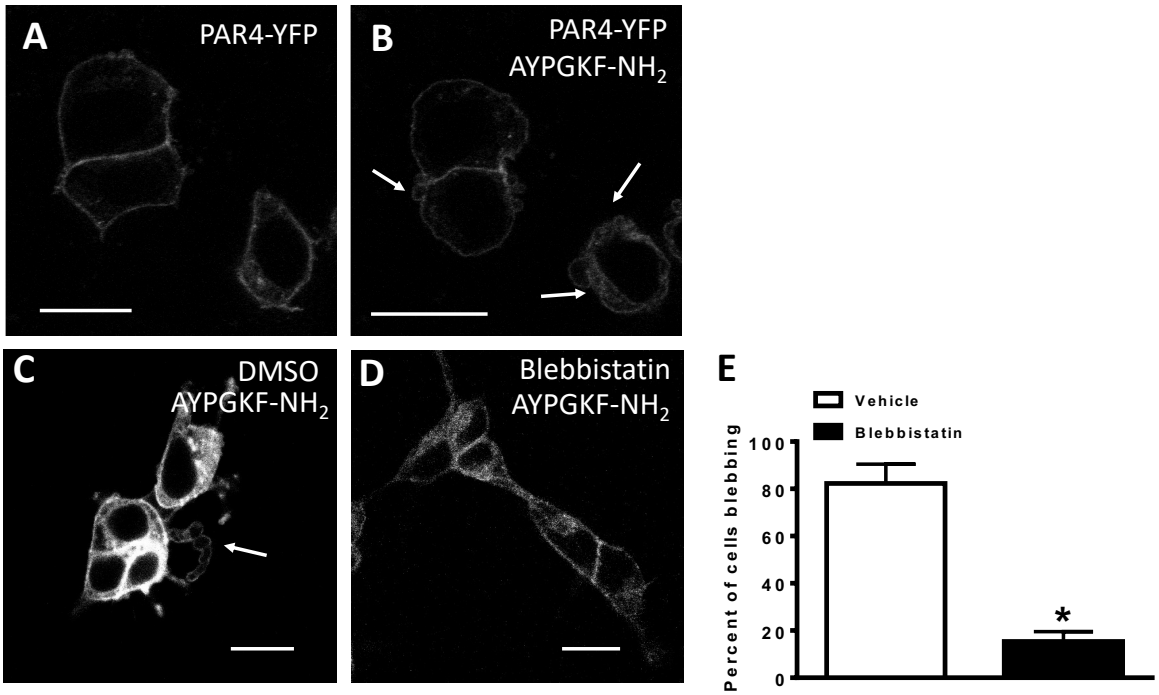

848
849

Figure 2:

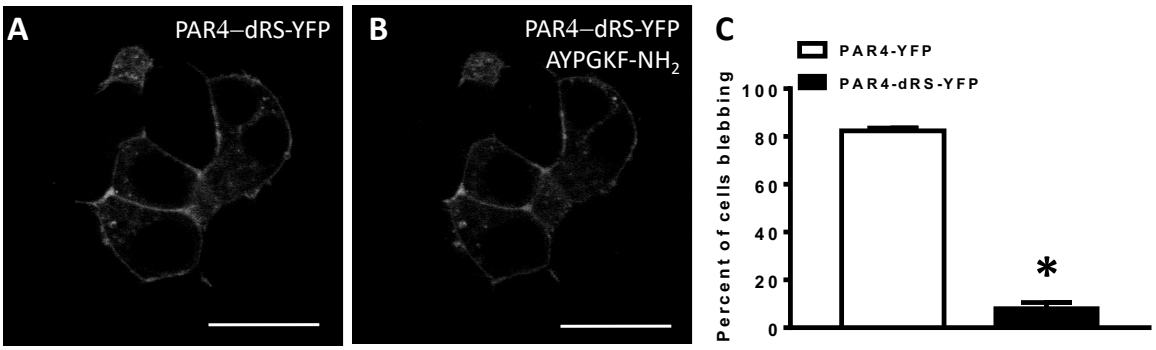

850
851
852

Figure: 3

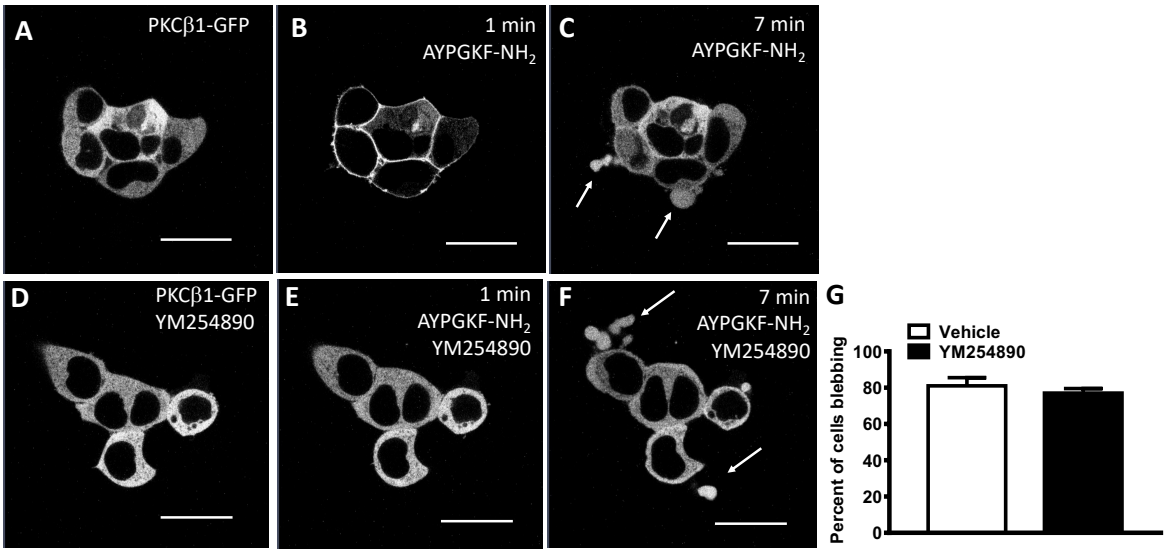

853
854

Figure 4:

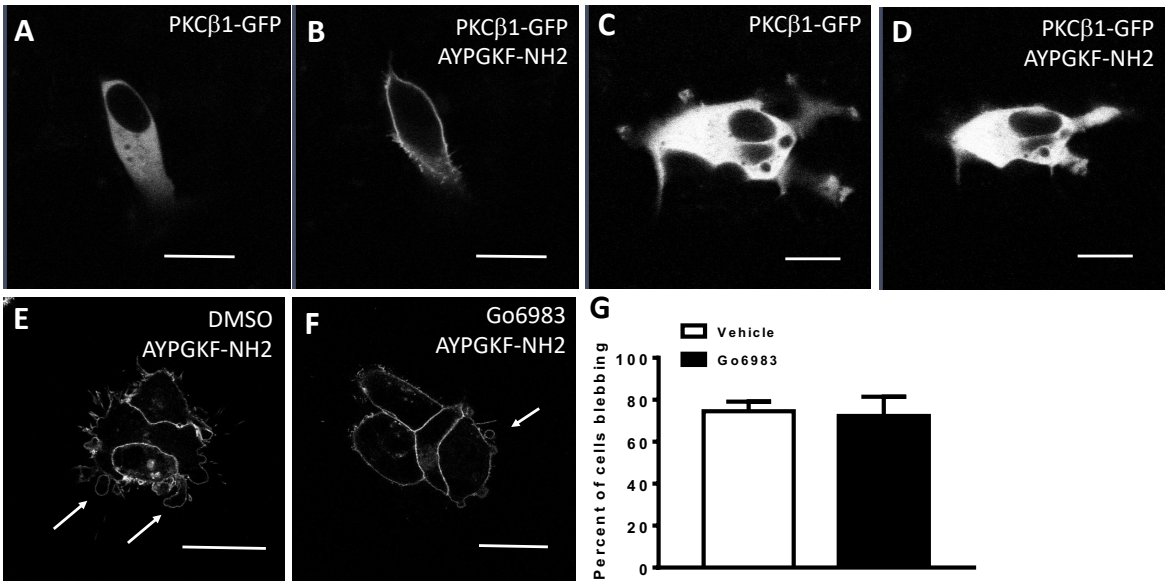

855
856

Figure 5:

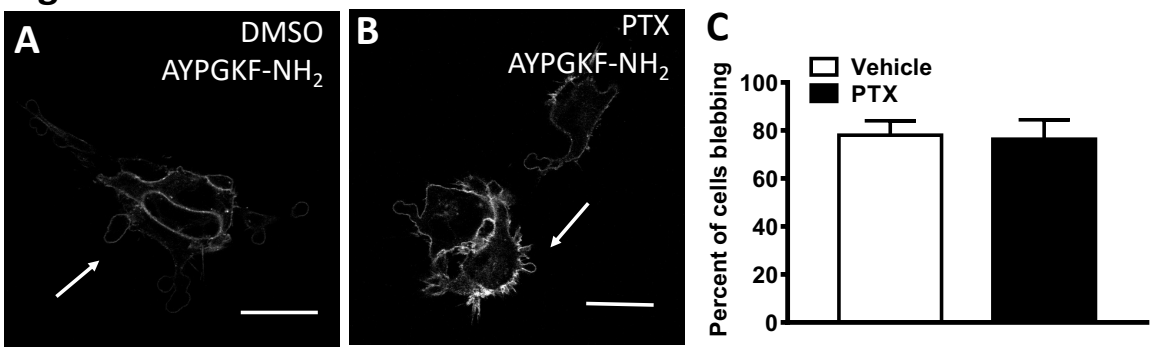

857
858

Figure 6:

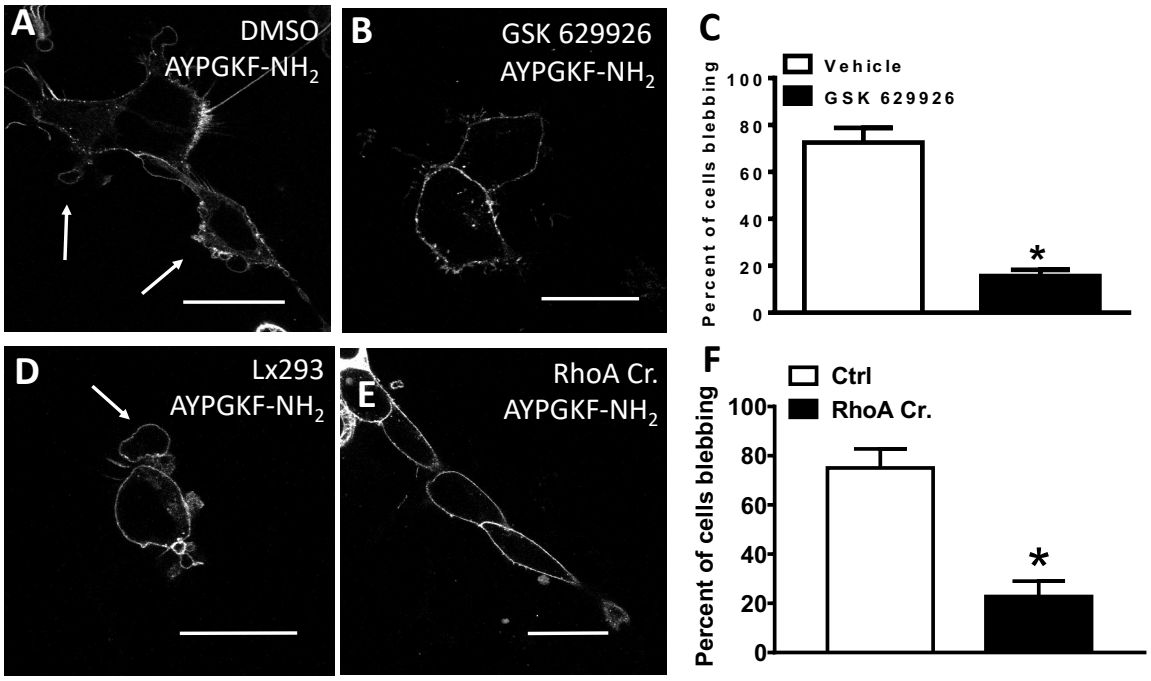
A
DMSO
AYPGKF-NH2
B
GSK 629926
AYPGKF-NH2
C
Vehicle
GSK 629926
Percent of cells blebbing
100
80
60
40
20
0
*
D
Lx293
AYPGKF-NH2
E
RhoA Cr.
AYPGKF-NH2
F
Ctrl
RhoA Cr.
Percent of cells blebbing
100
80
60
40
20
0
*

Figure: 7

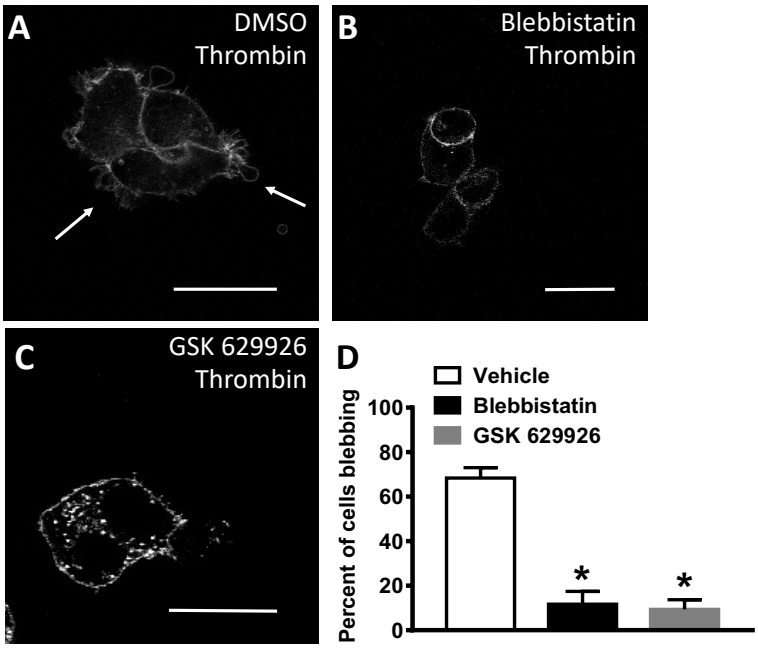

861
862

Figure 8:

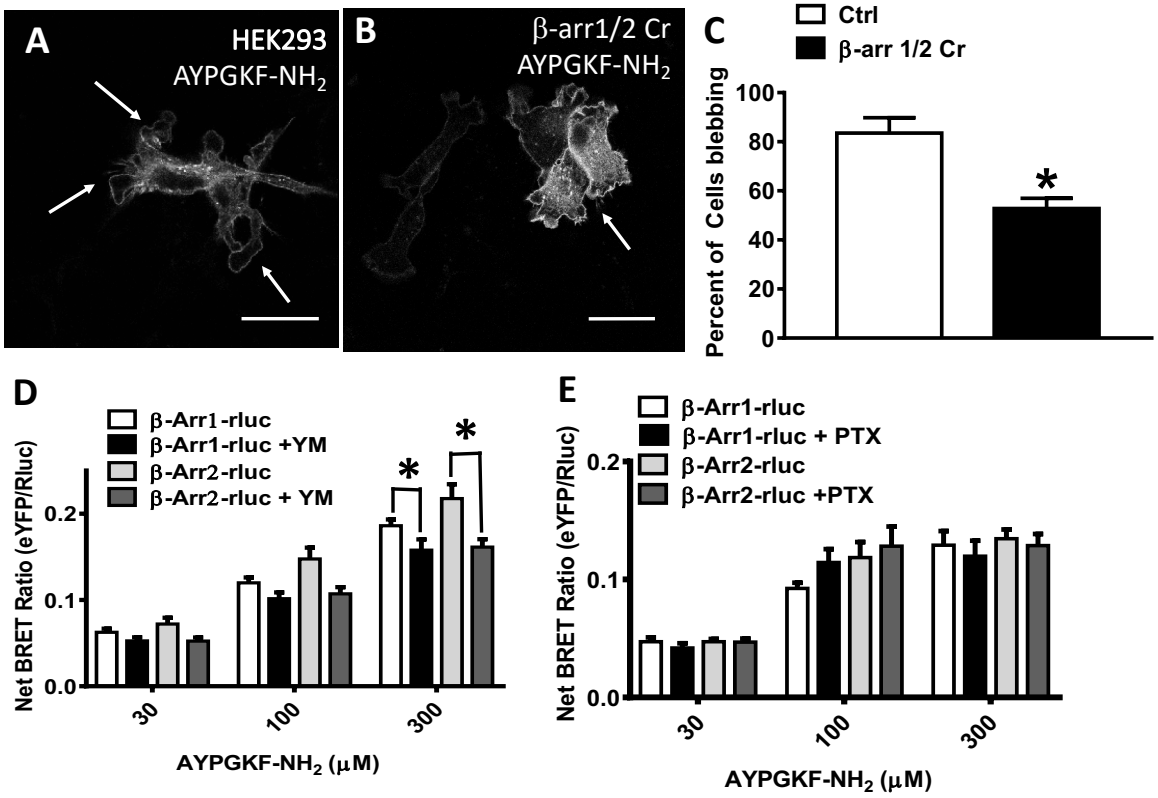

863
864
865

Figure 9:

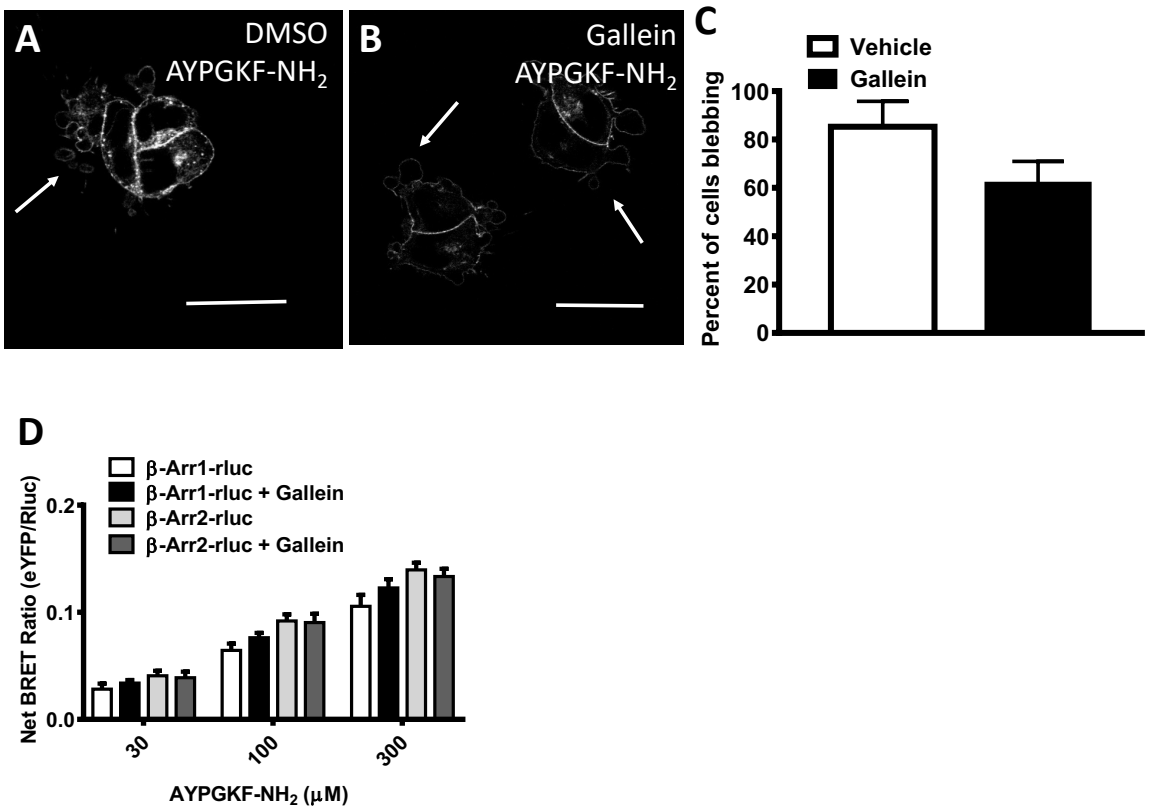

866
867

Figure 10:

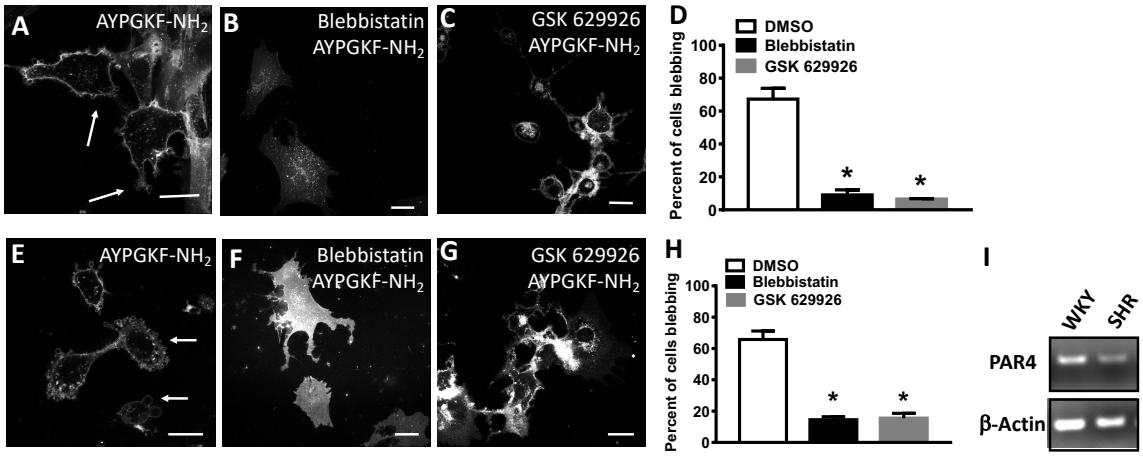
A
AYPGKF-NH2
B
Blebbistatin
AYPGKF-NH2
C
GSK 629926
AYPGKF-NH2
D
DMSO
Blebbistatin
GSK 629926
Percent of cells blebbing
100
80
60
40
20
0
*
*
E
AYPGKF-NH2
F
Blebbistatin
AYPGKF-NH2
G
GSK 629926
AYPGKF-NH2
H
DMSO
Blebbistatin
GSK 629926
Percent of cells blebbing
100
80
60
40
20
0
*
*
I
WKY
SHR
PAR4
β-Actin

Table 1:

A

Gene Ontology Term	Fold Enrichment
Neuron-neuron synaptic transmission (GO:0007270)	7.69
Natural killer cell activation (GO:0030101)	5.45
Fertilization (GO:0009566)	4.68
Sensory perception of taste (GO:0050909)	4.11
Blood coagulation (GO:0007596)	3.1
Cell-cell adhesion (GO:0016337)	2.81
Sensory perception of chemical stimulus (GO:000760	2.8
Macrophage activation (GO:0042116)	2.78
Blood circulation (GO:0008015)	2.73
Sensory perception (GO:0007600)	2.63

B

Gene Ontology Term	Fold Enrichment
JNK cascade (GO:0007254)	7.88
Anatomical structure morphogenesis (GO:0009653)	3.85
Death (GO:0016265)	3.06
Cell death (GO:0008219)	3.06
Apoptotic process (GO:0006915)	3.01
Intracellular signal transduction (GO:0035556)	2.89
Immune system process (GO:0002376)	2.77
Cell cycle (GO:0007049)	2.36
Developmental process (GO:0032502)	2.22
Signal transduction (GO:0007165)	1.72

870
871

Supplemental Figure 1:

RhoA#1 CGAGTTTGCGACTCGCGGAC
RhoA#2 CGGTCCGCGAGTCGCAAACT
RhoA #3 GAGTCCAGCCTCTTCGCGCC
RhoA #4 GACTCGCGGACCGGCGTCCC

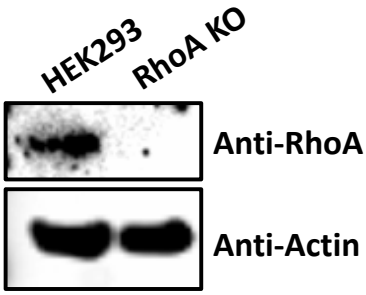

β-Arr 1 TGTGGACCACATCGACCTCG
β-Arr 2 GCGGGACTTCGTAGATCACC

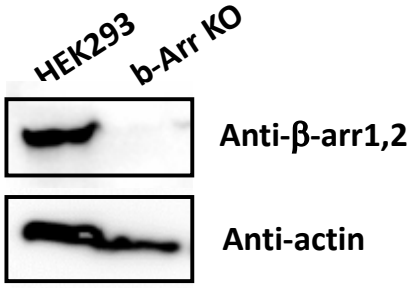

872
873
874

Supplemental Figure 2:

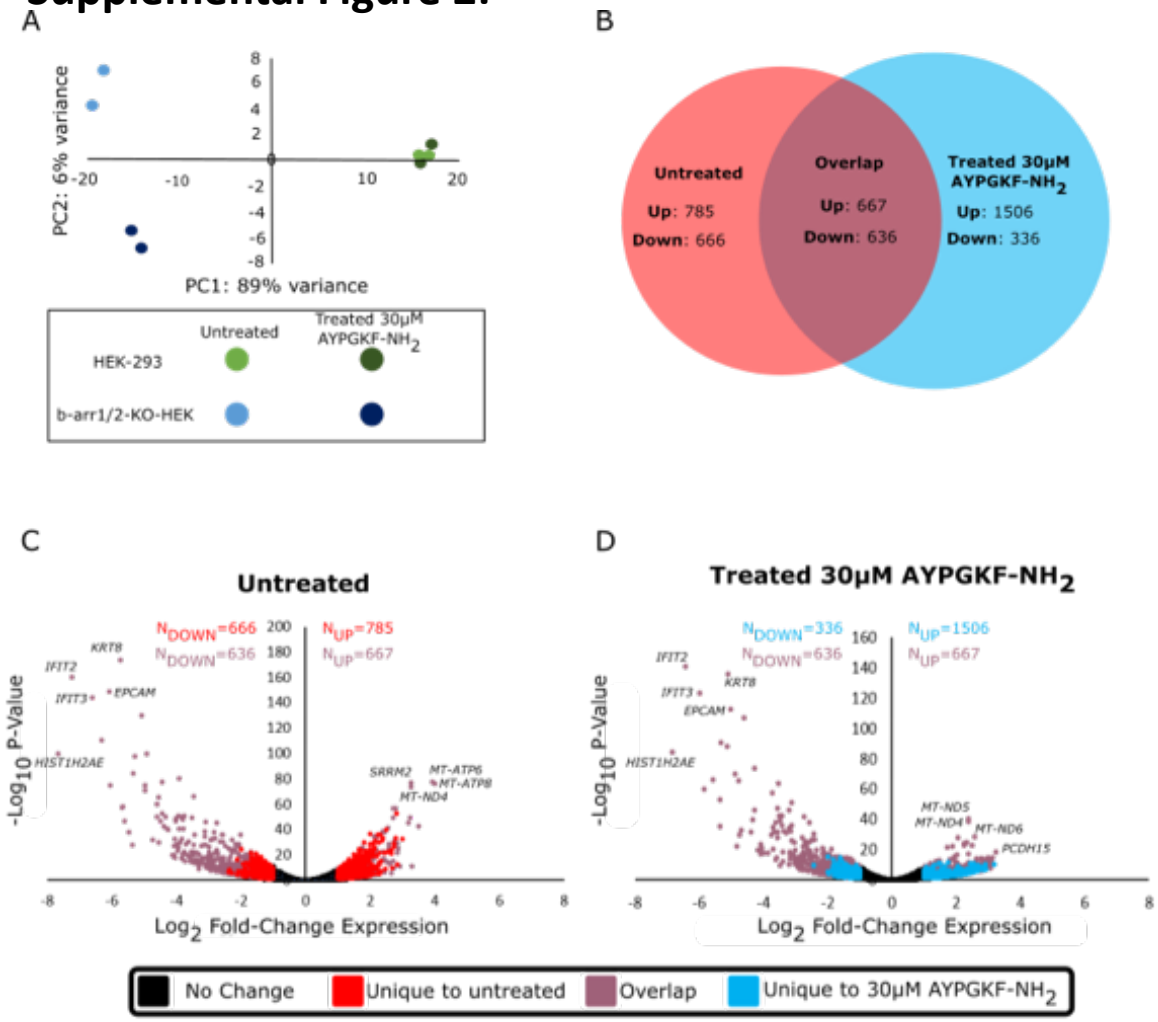

875